Int. J. Electrochem. Sci., 14 **(2019)** 11445 – 11455, doi: 10.20964/2019.12.71

International Journal of
ELECTROCHEMICAL
SCIENCE
www.electrochemsci.org

A Novel Photoelectrochemical Glucose Sensor Based on Graphene-CdS Nanocomposites Decorated with CoO_x Nanosheets

Zhimin Ma, Sujuan Li[*]

Henan Province Key Laboratory of New Optoelectronic Functional Materials, College of Chemistry and Chemical Engineering, Anyang Normal University, Anyang, 455000, Henan, China
[*]E-mail: lemontree88@163.com

Received: 7 July 2019 / *Accepted:* 24 September 2019 / *Published:* 29 October 2019

In this work, visible light driven enzyme-free glucose PEC sensor was developed by electrochemically deposited CoO_x nanosheets on graphene-CdS nanocomposites modified electrode to achieve both the electrocatalytic and photoelectrocatalytic oxidation of glucose at the resultant CoO_x/graphene-CdS nanocomposites modified electrode. Scanning electron microscopy, electrochemical impedance spectroscopy and cyclic voltammetry were used to characterize the morphology and electrochemical properties of the resultant CoO_x/graphene-CdS nanocomposites. The CV results demonstrated that decoration of CoO_x nanosheets largely enhanced the photoelectrocatalytic activity of graphene-CdS composites toward glucose oxidation in alkaline solution. The glucose detection sensitivity under visible light irradiation is dramatically improved compared to dark condition. Good performance was obtained for the CoO_x/graphene-CdS nanocomposites based glucose sensor. The feasibility of the present method was confirmed by good recovery results for glucose detection in human urine samples.

Keywords: Graphene; CdS nanowires, Cobalt oxide nanosheet, Glucose, Photoelectrochemical sensor.

1. INTRODUCTION

Glucose plays important roles in various fields, such as food industries, pharmaceutical, industrial and envionmental analysis, biofuel cells and clinical diagnostics [1-3]. In addition, a higher glucose level is found in human serum sample with diabetes [4,5], and presence of glucose in urine samples is related with kidney disease. Thus, developing sensitive and accurate glucose detection method is urgently needed. Various materials have been used to fabricate enzymatic and non-enzymatic glucose sensors [6-11]. Enzymatic sensors have high detection sensitivity and selectivity toward glucose detection, but is limited by the high cost and instability of enzymes due to its activity being easily affected by temperature, pH and ionic strength. Recently, non-enzymatic glucose sensors

have been a hot research topic and exploiting novel nanomaterials for direct electrocatalytic oxidation of glucose is a significant challenge.

Cobalt based nanomaterials show potential applications in areas of energy storage system, electrochromic devices and analytical sensors arising from its advantages of facile compatibility, good conductivity, low cost and high electrocatalytic activities [12-15]. Cobalt based nanomaterials have been reported to exhibit excellent electrocatalytic effect toward a range of small molecules, such as H_2O_2 [16,17], nitrite [18] and glucose [15,19] under the mediated reaction of different valance of Co. Various cobalt oxides (CoO_x) including Co_3O_4 [19], CoOOH [20] and so on have been synthesized as effective electrocatalysts. However, the performance of the present CoO_x based sensor for detection of glucose need to be further improved.

As we all known, apart from enzymatic catalysis and electrocatalysis, glucose can also be oxidized by photocatalysis on photoactive materials such as TiO_2 [21-23], WO_3 [24,25], MoS_2 [26,27], ZnO [28] and CdS [29] nanomaterials. Photoelectrochemical (PEC) measurement, coupling photoirradiation with electrochemical detection system, is characterized by ultrahigh sensitivity and low background signal. PEC has been developed as a powerful strategy for glucose sensing analysis. In PEC system, photoactive materials with excellent optoelectronic properties were vital for constructing high-performance photovoltaic devices. Among various semiconducting nanomaterials, CdS with a narrow band gap of 2.4 eV, is one of the most widely studied photoactive materials in the PEC synstem under visible light irradiation. However, the separation efficiency of photogenerated electron-hole pair's is low [29]. Modification of CdS with highly conductive materials such as graphene is the commonly used strategy to promote the charge separation and thus enhance the photovoltaic conversion efficiency of CdS [30].

In the present work, visible light driven enzyme-free glucose PEC sensor was developed by electrochemically deposited CoO_x nanosheets on graphene-CdS nanocomposites modified electrode to achieve both the electrocatalytic and photoelectrocatalytic oxidation of glucose at the resultant CoO_x/graphene-CdS nanocomposites modified electrode. For this nanocomposites, CdS nanowires (CdS NWs) were first synthesized by hydrothermal method, and then was further functionalized with amino groups to make it positively charged. Then, CdS NWs were incorporated with graphene oxide (GO) through electrostatic assembly. After a thermal reduction process, graphene-CdS composites were obtained. CoO_x nanosheets were subsequently electrodeposited onto glassy carbon electrode (GCE) modified with graphene-CdS by potential cycling in a solution with Co^{2+} involved. The electrocatalytic and photoelectrocatalytic activity of obtained CoO_x/graphene-CdS nanocomposites toward glucose oxidation was investigated in dark and under visible-light irradiation, respectively. The fabricated CoO_x/graphene-CdS nanocomposites modified electrode exhibited higher photo-electrocatalytic activity toward glucose oxidation than graphene-CdS under visible light illumination. In addition, an enhanced electrochemical response of CoO_x/graphene-CdS nanocomposites for glucose under visible-light irradiation was obtained compared to that in dark condition. Therefore, an enzyme-free photoelectrochemical glucose sensor with high performance based on CoO_x/graphene-CdS nanocomposites was demonstrated.

2. EXPERIMENTAL SECTION

2.1. Reagents and apparatus

GO was purchased from Nanjing XFNANO Materials Tech Co., Ltd. 3-aminopropyl-trimethoxysilane (APTMS), glucose and interference species were purchased from Sigma-Aldrich. Sodium diethyldithiocarbamate trihydrate ($C_5H_{10}NNaS_2 \cdot 3H_2O$), $CoCl_2$, $CdCl_2$ and NaOH were purchased from Aladdin Chemical Reagent Co. All of these reagents were of analytical grade and used as received.

The surface morphology of synthesized materials were characterized by scanning electron microscopy (SEM) using Hitachi SU8010 (Japan) for observations. Electrochemical experiments containing electrochemical impedance spectroscopy (EIS), cyclic voltammetry (CV) and amperometric technique were conducted on a CHI 660D electrochemical station (Shanghai Chenhua) with a conventional three-electrode system. The CoO_x/graphene-CdS nanocomposites modified glassy carbon electrode (CoO_x/graphene-CdS/GCE) was used as the working electrode. A saturated calomel electrode (SCE) and a Pt wire acted as the reference and counter electrodes, respectively. The electrochemical measurement under visible light irradiation was carried out in a quartz cell in the presence of three-electrode system under the irradiation of 300 W Xe lamp.

2.2. Preparation of graphene-CdS nanocomposites

Firstly, cadmium diethyldithiocarbamate was prepared by the reaction of $C_5H_{10}NNaS_2 \cdot 3H_2O$ and $CdCl_2$ to form precipitate. 1.124 g of the obtained precipitate was transferred into a 50 mL Teflon-lined stainless steel autoclave with the subsequent addition of 40 mL ethylenediamine. Afterwards, the autoclave was sealed and maintained at 180 ◦C for 24 h, and then allowed to cool down to room temperature naturally. The collected yellow sediment was rinsed with deionized water and ethanol to remove the residual solvent. After dried in 60 ◦C for 12 h, CdS NWs was obtained.

0.4 g of the resulting CdS NWs was dispersed into 200 mL ethanol and ultrasonicated for 30 min. Subsequently, 2 mL of APTMS was added and the mixture was heated to 60 ℃ for refluxing 4 h. The resultant APTMS functionalized CdS NWs was rinsed with absolute ethanol for three times. Through this process, positively charged CdS NWs was obtained.

The negatively charged GO solution was added into the above CdS NWs with a weight ration of 0.05：1. The pH of the mixture was adjusted to 6.0 and incubated for 30 min. Under electrostatic assembly, the GO-CdS nanocomposite was obtained. After that, 0.4 g of GO-CdS nanocomposite was added into an autoclave with 20 mL ethanol and 60 mL distilled waster involved. The autoclave was maintained at 120 ◦C for 12 h to get the graphene-CdS nanocomposites through the following rinsing and drying steps.

2.3. Preparation of CoO_x/graphene-CdS nanocomposites modified electrode

The GCE was pretreated by polishing with 0.3 and 0.05 μm alumina slurries respectively. The

electrode was placed in ethanol and water container under ultrasonic bathing to remove adsorbed particles. A 2 μL portion of the prepared graphene-CdS dispersion (5 mg/mL) was dropped onto a pretreated GCE and dried at room temperature to obtain the graphene-CdS/GCE. CoO_x nanosheets were then electrodeposited onto graphene-CdS/GCE by CV in electrolyte solutions with 10 mM $CoCl_2$ and 0.1 M KCl involved by scanning in the potential range of -1.1 to 1.1 V for 50 cycles at 100 mV s^{-1}. The direct electrodeposition of CoO_x nanosheets on bare GCE surface was denoted as CoO_x modified electrode (CoO_x/GCE) for comparison.

3. RESULTS AND DISCUSSION

3.1. Characterization of CoO_x/graphene-CdS nanocomposites

The morphology of the fabricated CdS NWs, graphene-CdS and CoO_x/graphene-CdS nanocomposites was characterized by SEM. As can be seen from Fig.1, the synthesized CdS NWs (Fig.1a) have a nanowire morphology with diameters of about 20~40 nm.

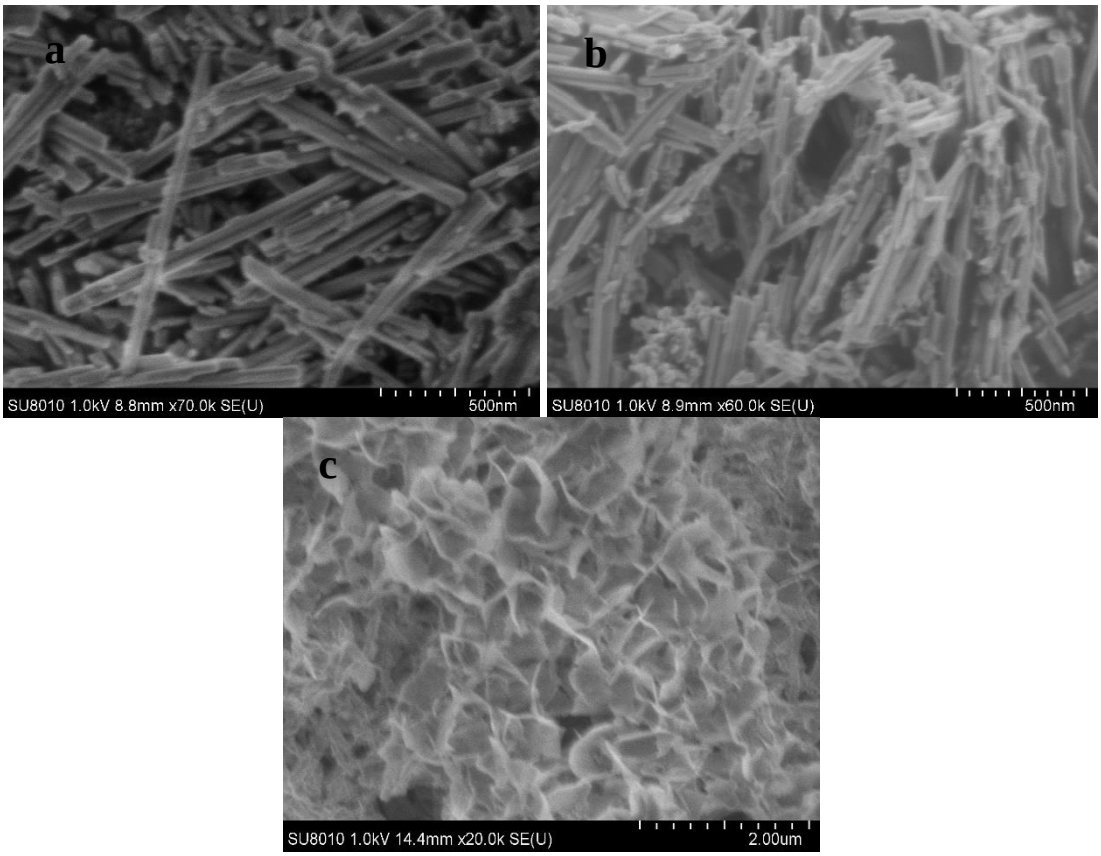

Figure 1. SEM images of CdS NWs (a), graphene-CdS (b) and CoO_x/graphene-CdS nanocomposites (c).

The length of CdS NWs can extends to 1 μm. After electrostatic assembly of CdS NWs with GO to form graphene-CdS composites (Fig.1b), 2D sheet-like morphology and 1D nanowires can both

be observed. For CoO_x/graphene-CdS nanocomposites (Fig.1c), CoO_x nanosheet structures were uniformly grown onto graphene-CdS surface. There are space within sheet to sheet to make the structure apparently more porous like. The porous nanosheet materials facilitate mass transport and enlarge the electrode surface area, which is benefiting for developing a high-performance glucose sensor.

The electrochemical properties of the obtained CoO_x/graphene-CdS nanocomposites modified electrode was investigated in alkaline solution by CV technique. Fig. 2a shows the CV responses of CoO_x/graphene-CdS/GCE in 0.1 M NaOH at a scan rate of 50 mV s^{-1}. Obviously, an distinct oxidation peak at 0.29 V relating to the conversion between different cobalt oxidation phases was observed. For the reverse scan, two cathodic peaks are located at 0.21 and 0.47 V, which corresponds to the reduction of preformed cobalt oxided species [16]. This result suggest the successful formation of CoO_x nanosheets on surface of graphene-CdS. The electrochemical reaction kinetics of CoO_x/graphene-CdS/GCE in alkaline solution was also investigated by CV scanning at different scan rates, the results of which is presented in Fig. 2b. As observed, both the oxidation and reduction peak currents increased with the increase of scan rates, and the redox peak currents are linearly proportional to scan rate (as presented in the inset of Fig. 2b), indicating the surface controlled process for electrochemical reaction of CoO_x/graphene-CdS nanocomposites.

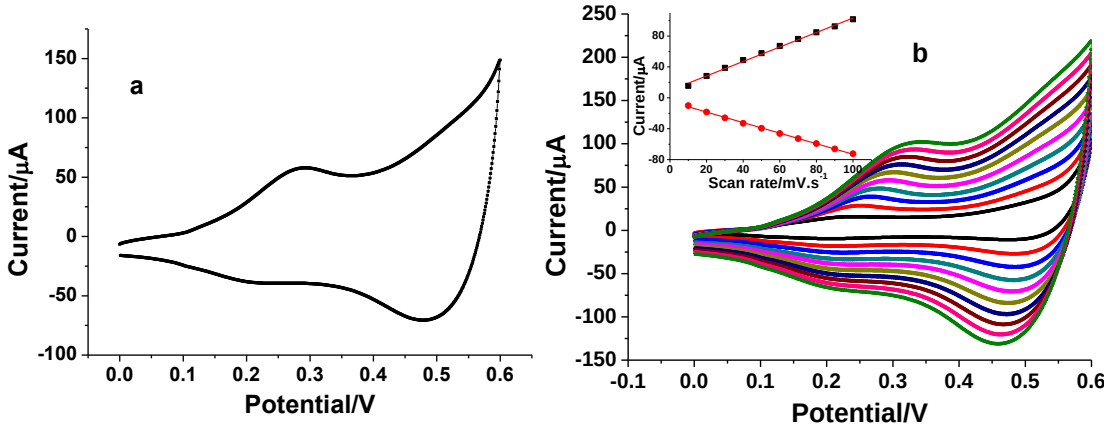

Figure 2. (a) CV response of CoO_x/graphene-CdS nanocomposites modified electrode in 0.1 M NaOH at a scan rate of 50 mV s^{-1}, and the influence of scan rate on the above CV response (b). The inset of fig.2b is the relationship between peak currents and scan rates.

EIS is a powerful tool for revealing the interface properties of modified electrodes. A typical EIS plot concludes a semi-circle part and a linear part. The diameter of the semi-circle part is corresponds to the electron transfer process (R_{et}). Fig. 3 shows the EIS of the bare GCE (a), graphene-CdS/GCE (b) and CoO_x/graphene-CdS/GCE (c) in 1 mM $Fe(CN)_6^{3-/4-}$ and 0.1 M KCl solution in the frequency range of 0.1 Hz-10 kHz. As illustrated, the bare GCE has the most small R_{et} value (558 Ω). The modification of graphene-CdS leads to an obvious increased R_{et} value (1714 Ω), suggesting that the immobilization of graphene-CdS composites blocks the interfacial electron transfer due to a thick layer of semi-comductive CdS NWs covered. With the subsequent electrodeposition of CoO_x nanosheets, the R_{et} value (3160 Ω) of the CoO_x/graphene-CdS/GCE further increased apparently

arising from the semiconducting properties of electrodeposited CoO_x nanosheets. In addition, the gradual increase of R_{et} value suggest the successful modification of graphene-CdS composites composites and CoO_x nanosheets on electrode surface.

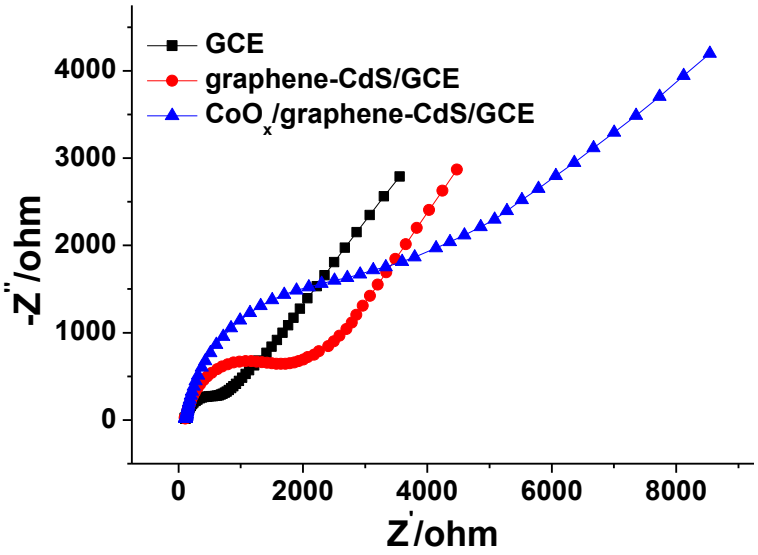

Figure 3. EIS of the bare GCE (a), graphene-CdS/GCE (b) and CoO_x/graphene-CdS /GCE (c) in 1 mM $Fe(CN)_6^{3-/4-}$ and 0.1 M KCl solution in the frequency range of 0.1 Hz-10 kHz.

3.2. Electrocatalytic oxidation of glucose on the CoO_x/graphene-CdS/GCE

The electrocatalytic activity of CoO_x/graphene-CdS nanocomposites toward glucose oxidation in an alkaline media was investigated by CV method. For comparison, CoO_x/GCE and graphene-CdS/GCE were also studied. Fig. 4 exhibits the CV responses of the CoO_x/GCE (a), graphene-CdS/GCE (b) and CoO_x/graphene-CdS/GCE (c) in 0.1 mol/L NaOH with the absence and presence of 1 mM glucose in dark and under visible light irradiation. As seen from Fig. 4(a), the addition of glucose caused an obvious increase for anodic current from a potential of 0.3 V at CoO_x/GCE due to prominent electrocatalytic activity of CoO_x toward the oxidation of glucose [19]. After exposing to visible light, there is a tiny change in the anodic current, which indicates poor photo-activity of CoO_x under visible light illumination [31]. For graphene-CdS/GCE (b), the glucose addition resulted no change in the anodic current. However, an obvious increase of anodic current can be fund under visible light irradiation. This result indicates the electrocatalytic inactivity of graphene-CdS but photo-activity toward glucose oxidation because of the generation of hole-electron pairs in graphene-CdS composite. For CoO_x/graphene-CdS/GCE (c), the addition of glucose results in a distinct increase for anodic current from a potential of 0.3 V, the visible light illumination further increase the anodic current significantly. This result suggest both the electrocatalytic and photocatalytic activities of CoO_x/graphene-CdS composite toward glucose oxidation. Compared Fig. 4b and Fig. 4c, the anodic current response caused by glucose oxidation at CoO_x/graphene-CdS composite is significantly larger than that at only graphene-CdS, which indicates that decoration of CoO_x nanosheets dramatically

enhanced photoelectrocatalytic activities of graphene-CdS composites toward glucose oxidation. Furthermore, as demonstrated in Fig. 4(d), the anodic currents from a potential of 0.3 V increased with increasing of glucose concentration, and a further increase was observed upon light irradiation. Based on the above results, it can be concluded that the CoO_x/graphene-CdS nanocomposite shows effective photoelectrochemical activity toward glucose oxidation.

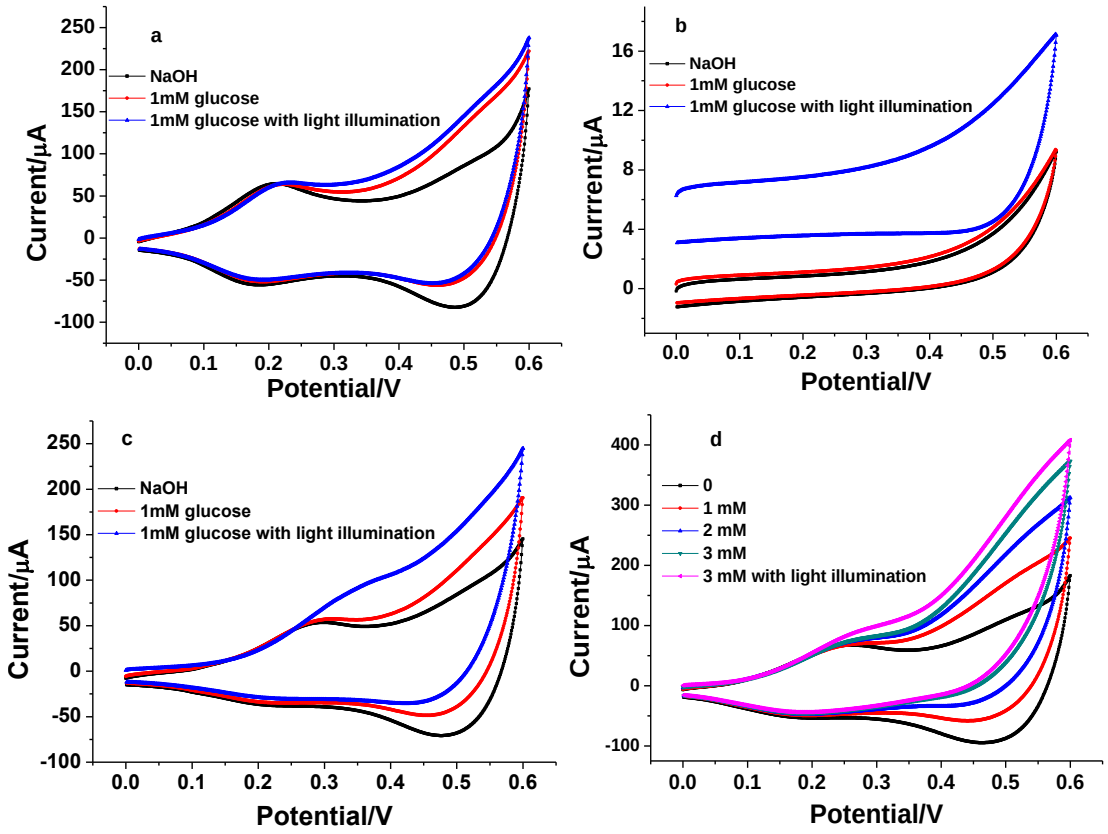

Figure 4. CV responses of the CoO_x/GCE (a), graphene-CdS/GCE (b) and CoO_x/graphene-CdS/GCE (c) in 0.1 mol/L NaOH with the absence (black curve) and presence (red curve) of 1 mM glucose in dark and under visible light irradiation (blue curve), (d) is the CVs of CoO_x/graphene-CdS/GCE in dark for 0, 1, 2 and 3 mM of glucose and for 3 mM of glucose under visible light irradiation.

3.3. Amperometric detection of glucose at CoO_x/graphene-CdS/GCE

The quantitative analysis of glucose was carried out by amperometric method. Fig.5(a) shows the amperometric responses of CoO_x/graphene-CdS/GCE holding at potential of 0.4 V for successive additions of different concentrations of glucose to 0.1 M NaOH solution in dark and under visible light irradiation. As found in fig.5(a), upon each addition of glucose, stable and stepwise current increases accordingly with the level of glucose and reaches a new equilibrium within 4 s. In addition, the amperometric current under light illumination is much larger than that in dark condition, indicating more sensitive response for glucose at CoO_x/graphene-CdS/GCE under the help of light illumination.

The inset of fig. 5(a) exhibits plots of current response *vs* glucose concentration. A nearly linear and sensitive response was found for the low concentration range of glucose, but the increasing rate for current response *vs* glucose concentration is lowered for higher concentration of glucose, probably due to the blocked actives sites of CoO_x/graphene-CdS naocomposites by the oxidation product of glucose [32]. The calibration curve of the present method is presented in Fig.5 (b). The obtained calibration equation can be expressed as I(μA)=1.47884+0.03594C (μM) with a correlation coefficient of 0.9951 in the dark condition, and I(μA)=1.55053+0.05629C (μM) with a correlation coefficient of 0.9970 under light illumination. The linear response range of glucose is 5-370 μM with a detection sensitivity of 508.7 μA mM^{-1} cm^{-2} and 796.7 μA mM^{-1} cm^{-2} in the dark and under visible light irradiation, respectively. A 1.57 times increase in sensitivity suggest an effective photoelectrochemical catalytic activity of CoO_x/graphene-CdS naocomposites toward glucose oxidation. The limit of detection (LOD) is calculated to be 0.7 μM and 0.5 μM in the dark and light irradiation, respectively.

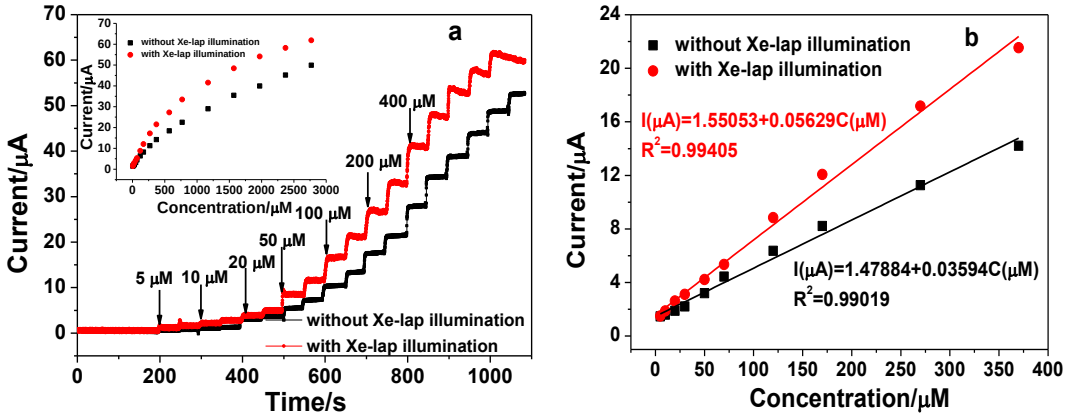

Figure 5. (a) Amperometric responses of CoO_x/graphene-CdS/GCE holding at potential of 0.4 V for successive additions of different concentrations of glucose to 0.1 M NaOH solution in dark and under visible light irradiation. The inset is plots of current response *vs* glucose concentration. (b) The calibration curve of the present method with the data obtained from Fig.5a.

Table 1. Comparison of the analytical performance of CoO_x/graphene-CdS based glucose sensor with other cobalt based nanomaterials.

Electrode materials	Potential (V)	Sensitivity (μA mM^{-1} cm^{-2})	Linear range (mM)	LOD (μM)	Ref.
Ni-Co oxide/rGO	0.42	548.9	0.005–8.6	2	33
3D graphene/Co_3O_4	0.58	3.39	<0.08	<0.025	34
rGO/CdS/CoOx	0.4	5900	0.001–0.01	0.4	31
CoO_x NPs/ERGO	0.6	79.3	0.01-0.55	1	35
CoO_x/graphene-CdS	0.4	796.7	0.005-0.37	0.5	This work

The comparison of the analytical performance of CoO_x/graphene-CdS based glucose sensor with other cobalt based nanomaterials is shown in Table 1. Obviously, the CoO_x/graphene-CdS based glucose sensor has comparable performance compared to other cobalt based nanomaterials as listed in

Table 1. The sensitivity of the present sensor is much larger than that for Ni-Co oxide/rGO composites [33] and 3D graphene/Co_3O_4 [34] and CoO_x nanoparticles (NPs)/electrochemcially reduced graphene oxide (ERGO) [35]. The similar materials prepared by CoO_x finny ball nanostructures decorated rGO/CdS NPs [31] shows a distinct higher sensitivity, the linear concentration range is significantly narrower compared to the present CoO_x nanosheets decorated graphene-CdS NWs.

3.4. Selectivity of the CoO_x/graphene-CdS based glucose sensor

Anti-interference ability is an important factor for evaluating a highly efficient glucose sensor. Some compounds such as H_2O_2, ascorbic acid (AA), dopamine (DA) and uric acid (UA) that are prone to be oxidized are usually found to coexist with glucose and interfere with the detection of glucose. Cl^- is also reported to posion the sensing surface [31]. Thus, the anti-interference ability of the present CoO_x/graphene-CdS based glucose sensor under the presence of the above mentioned substance was evaluated. Since the normal amount of glucose in human blood (3-8 mM) is nearly 10 times higher than those of DA, AA, UA [32], the molar ratio of 1:10 for glucose and interferences was exploited to perform anti-interference experiment. Fig. 6 shows amperometric responses of CoO_x/graphene-CdS/GCE for successive additions of 0.5 mM glucose, 0.05 mM H_2O_2, 0.05 mM NaCl, 0.05 mM dopamine (DA), 0.05 mM ascorbic acid (AA), 0.05 mM uric acid (UA) and 0.5 mM glucose to 0.1 M NaOH solution under visible light irradiation. It can be found that H_2O_2, NaCl and UA generate no current response compared to glucose. DA and AA caused a current response less than 10% of that of glucose. This results suggest acceptable selectivity of CoO_x/graphene-CdS/GCE for glucose detection.

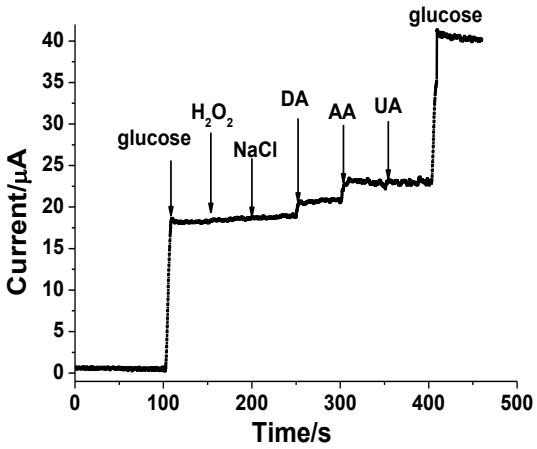

Figure 6. Amperometric responses of CoO_x/graphene-CdS/GCE for successive additions of 0.5 mM glucose, 0.05 mM H_2O_2, 0.05 mM NaCl, 0.05 mM dopamine (DA), 0.05 mM ascorbic acid (AA), 0.05 mM uric acid (UA) and 0.5 mM glucose to 0.1 M NaOH solution under visible light irradiation.

3.5. Analysis of glucose in human urine samples

The feasibility of the CoO_x/graphene-CdS/GCE for glucose detection was evaluated in human

urine samples. There was no glucose found in two human urine samples. A certein concentration of glucose was spiked in the above two urine samples. Standard addition method was applied for glucose monitoring in human urine samples. The determination results are shown in Table 2. As observed, the recoveries for glucose are in the range of 96.5%-104%, revealing that the feasibility of the present method for analysis of glucose in real samples.

Table 2. Determination results for glucose in human urine sample.

Spiked urine sample (μM)	Added (μM)	Detected (μM)	Recovery (%)
50	100	154	104
100	200	293	96.5

4. CONCLUSIONS

In summary, a novel enzyme-free photoelectrochemical glucose sensor based on graphene-CdS nanocomposites via decoration of CoO_x nanosheets was demonstrated. The resultant CoO_x/graphene-CdS modified electrode shows good electrocatalytic activity toward glucose oxidation in dark condition, and if under visible light irradiation, the electrochemical current is further enhanced significantly due to photoelectrocatalytic activity of CoO_x/graphene-CdS/GCE nanocomposites. The CV results demonstrated that decoration of CoO_x nanosheets dramatically enhanced photoelectrocatalytic activities of graphene-CdS composites toward glucose oxidation. As an enzyme-free photoelectrochemical glucose sensor, excellent performance including a high sensitivity (796.7 μA mM^{-1} cm^{-2}), wide linear concentration range (0.005-0.37 mM), low detection limit (0.5 μM) and good selectivity was obtained for CoO_x/graphene-CdS composites. The present method for detection of glucose in real human urine sample demonstrated good recovery results, suggesting the validity of the present method for effective glucose monitoring.

ACKNOWLEDGMENTS
This work was supported by the Grants from the National Natural Science Foundation of China (21105002, U1704135), the Technology Development Plan Project for Anyang City (21).

References

1. J. Wang, *Chem. Rev*., 108 (2008) 814.
2. N.A. Rakow and K.S. Suslick, *Nature*, 406 (2000) 710.
3. J. Wang, *Electroanalysis*, 17 (2005) 7.
4. A. Heller and B.Feldman, *Acc. Chem. Res*., 43 (2010) 963.
5. M. Zhang, P. Yu and L. Mao, *Acc. Chem. Res*. 45 (2012) 533.
6. S.J. Li, T.W. Chen, N. Xia, Y.L. Hou, J.J. Du and L. Liu, *J. Solid State Electrochem*., 17 (2013) 2487.
7. S.J. Li, N. Xia, X.L. Lv, M.M. Zhao, B.Q. Yuan and H. Pang, *Sens. Actuators B*, 190 (2014) 809.

8. S.J. Li, Y. Xing, L.L. Hou, Z.Q. Feng, Y. Tian and J.M. Du, *Int. J. Electrochem. Sci*., 11 (2016) 6747.
9. S.J. Li, W. Guo, R.T. Liu and J.M. Du, *Int. J. Electrochem. Sci*., 11 (2016) 7690.
10. L. Wang, Y. Zhang, J. Yu, J. He, H. Yang, Y. Ye and Y. Song, *Sens. Actuators B*, 239 (2017) 172.
11. X. Chen, G. Wu, Z. Cai, M. Oyama and X. Chen, *Microchim. Acta*, 181 (2014) 689
12. H.J. Qiu, L. Liu, Y.P. Mu, H.J. Zhang and Y. Wang, *Nano Res*., 8 (2015) 321.
13. X.H. Xia, J.P. Tu, J. Zhang, J.Y. Xiang, X.L. Wang and X.B. Zhao, *Appl. Mater. Interfaces*, 2 (2010) 186.
14. V. Srinivasan and J.W. Weidner, *J. Power Sources*, 108 (2002) 15.
15. X.C. Dong, H. Xu, X.W. Wang, Y.X. Huang, M.B. Chan-Park, H. Zhang, L.H. Wang, W. Huang, and P. Chen, *ACS Nano*, 6 (2012) 3206.
16. A. Salimi, R. Hallaj, S. Soltanian and H. Mamkhezri, *Anal. Chim. Acta*, 594 (2007) 24.
17. J. Xu, J. Cai, J. Wang, L. Zhang, Y. Fan, N. Zhang, H. Zhou, D. Chen,Y. Zhong, H. Fan, H. Shao, J. Zhang and C. Cao, *Electrochem. Commun*., 25 (2012) 119.
18. Z. Meng, B. Liu, J. Zheng, Q. Sheng and H. Zhang, *Microchim. Acta*, 175 (2011) 251.
19. C. Hou, Q. Xu, L. Yin and X. Hu, *Analyst*, 137 (2012) 5803
20. K.K. Lee, P.Y. Loh, C.H. Sow and W.S. Chin, *Electrochem. Commun*., 20 (2012) 128.
21. Y. Yang, K. Yan and J. Zhang, *Electrochim. Acta*, 228 (2017) 28.
22. Y. Wang, L. Bai, Y. Wang, D. Qin, D. Shan, X. Lu, *Analyst*, 143 (2018) 1699.
23. L. He, Q. Liu, S. Zhang, X. Zhang, C. Gong, H. Shu, G. Wang, H. Liu, S. Wen, B. Zhang, *Electrochem. Commun*., 94 (2018) 18.
24. A. Devadoss, P. Sudhagar, S. Das, S.Y. Lee, C. Terashima, K. Nakata, A. Fujishima, W. Choi, Y.S. Kang, and U. Paik, *ACS Appl. Mater. Interfaces*, 6 (2014) 4864.
25. B. Zhang, Q. Zhang, L. He, Y. Xia, F. Meng, G. Liu, Q. Pan, H. Shu, C. Gong, F. Cheng, H. Liang, S. Wen, J. Electrochem. Soc., 166 (2019) B569.
26. S. Wu, H. Huang, M. Shang, C. Du, Y. Wu and W. Song, *Biosens. Bioelectron*., 92 (2017) 646.
27. J. Peng and J. Weng, *Biosens. Bioelectron*., 89 (2017) 652.
28. C.L. Hsu, J.H. Lin, D.X. Hsu, S.H. Wang, S.Y. Lin and T.J. Hsueh, *Sens. Actuators B*, 238 (2017) 150.
29. X. Zhao, S. Zhou, Q. Shen, L.P. Jiang and J.J. Zhu, *Analyst*, 137 (2012) 3697.
30. R. Bera, S. Kundu and A. Patra, *ACS Appl. Mater. Interfaces*, 7 (2015) 13251.
31. M. Ashrafi, A. Salimi and A. Arabzadeh, *J. Electroanal. Chem*., 783 (2016) 233.
32. S.J. Li, W. Guo, B.Q. Yuan, D.J. Zhang, Z.Q. Feng and J.M. Du, *Sens. Actuators B*, 240 (2017) 398.
33. G. Ma, M. Yang, C. Li, H. Tan, L. Deng, S. Xie, F. Xu, L. Wang and Y. Song, *Electrochim. Acta*, 220 (2016) 545.
34. X.C. Dong, H. Xu, X.W. Wang, Y.X. Huang, M.B. Chan-Park, H. Zhang, L.H. Wang, W. Huang and P. Chen, *ACS Nano*, 6 (2012) 3206.
35. S.J. Li, J.M. Du, J. Chen, N.N. Mao, M.J. Zhang and H. Pang, *J. Solid State Electrochem*, 18 (2014) 1049.